Available online at www.sciencedirect.com
SCIENCE DIRECT®
Chemical Physics Letters 402 (2005) 233–238
CHEMICAL PHYSICS LETTERS
www.elsevier.com/locate/cplett

Time resolved photoluminescence anisotropy of CdSe/ZnS nanoparticles in toluene at 300 K

E.P. Petrov [a,b,c], F. Cichos [a], E. Zenkevich [b], D. Starukhin [a,d], C. von Borczyskowski [a,*]

[a] Institute of Physics, Chemnitz University of Technology, Reichenhainerstrasse 70, DE-09107 Chemnitz, Germany
[b] B. I. Stepanov Institute of Physics, National Academy of Science of Belarus, Minsk 220072, Belarus
[c] Institute for Biophysics/BioTec, Dresden University of Technology, 01307 Dresden, Germany
[d] Institute of Physical Chemistry, University of Heidelberg, 69120 Heidelberg, Germany

Received 1 October 2004; in final form 30 November 2004

Abstract

For CdSe nanoparticles it has been theoretically and experimentally shown that at low temperatures the photoluminescence is circularly polarized in accordance with a wurtzite structure and the corresponding allowed optical transitions. In the present Letter, we report on related investigations on CdSe/ZnS colloids in toluene solution. From time resolved photoluminescence anisotropy we conclude that also at room temperature the results are in good agreement with structure and related electronic states as determined from crystals at low temperature.

1. Introduction

Theoretical calculations [1] predict that the prolate shape and the unidirectional wurtzite crystal structure of CdSe nanoparticles should result in two possible radiative transitions for band edge states. The energetically lowest lying transition is an electric dipole transition with the transition dipole moment oriented along the wurtzite *c*-axis. However, this transition is optically forbidden. The higher-lying optically allowed transition is predicted to be doubly degenerate and should give rise to an isotropic two-dimensional transition dipole lying within the crystallographic *a,b*-plane. Thus, if the observed nanocrystal photoluminescence (PL) is due to this transition, emission of an individual nanocrystal should be circularly (or, in case of deviation from perfect symmetry, elliptically) polarized. This was indeed recently observed in experiments with single nanocrystals [2–5]. Low-temperature (1.5–10 K) experiments with ensembles of CdSe nanocrystals [6] have also directly confirmed the circular polarization of the luminescence.

Up to now, no results have been published in the nanosecond range on the time dependence of the PL anisotropy of semiconductor nanoparticles solvated in liquids at room temperature. The previous room temperature studies of the time resolved anisotropy of TOPO-capped CdSe nanoparticles were carried out on the 10-ps time scale and showed no time dependence of the emission anisotropy in this regime [7]. In another study [8] no detectable steady-state and time resolved anisotropy was found for polyphosphate-stabilized CdS nanoparticles, whereas CdS nanoparticle/starburst dendrimer composites showed polarized room-temperature PL with the anisotropy characterized by an initial value of about 0.2 and a correlation time of about 2.4 μs.

* Corresponding author. Fax: +49 371 531 3060.
E-mail address: borczyskowski@physik.tu-chemnitz.de (C. von Borczyskowski).
URL: http://www.tu-chemnitz.de/physik/OSMP/.

0009-2614/$ - see front matter © 2004 Elsevier B.V. All rights reserved.
doi:10.1016/j.cplett.2004.12.036

However, extending investigations also to room temperature would help to improve the understanding of the relaxation pathways of excitons in nanocrystals. In particular, we will contribute in this Letter to this still open field in answering two questions: (i) Can the depolarization of nanocrystal luminescence in solution be explained by rotational diffusion of nanocrystals and (ii) Does selective excitation of nanocrystals at the red edge and thus on size selected particles within the absorption spectrum result in polarization properties of the luminescence? To proceed, time resolved PL anisotropy decays of CdSe/ZnS nanocrystals in toluene were investigated at 300 K as a function of both excitation and emission wavelength.

2. Experimental

Nanocrystals have been prepared according to [9]. Experiments were carried out at 300 K with toluene solutions of CdSe nanoparticles capped with three monolayers of ZnS. According to the position of the first excitonic absorption maximum (554 nm), the CdSe core diameter was estimated to be 3.2 nm. Based on the data from Schmelz et al. [10], the estimation of the molar extinction at 554 nm is 1.25×10^5 M^{-1} cm^{-1}. The concentration of CdSe/ZnS nanoparticles used in the present study was adjusted to 3.5 μM.

Optical absorption spectra were recorded on a Shimadzu UV-3101PC UV–VIS–NIR scanning spectrophotometer with a resolution of 1 nm. Steady-state fluorescence emission spectra were recorded on a Shimadzu RF-5001PC spectrofluorophotometer with a spectral resolution of 1.5 nm. Prior to carrying out steady-state fluorescence experiments, the spectrofluorophotometer was calibrated for the spectral response of the detection channel against a set of fluorescence standards according to the procedure described recently [11]. Relative fluorescence quantum yield measurements were carried out according to a conventional method [12]. A solution of Rhodamine 101 in acidic ethanol was used as fluorescent standard with the temperature-independent quantum yield close to 1.0 [13–15].

Time resolved fluorescence measurements were performed in the time-correlated single photon counting (TCSPC) mode under right-angle geometry. A cavity-dumped dye laser (Spectra-Physics Models 375B and 344S) with Rhodamine 6G in ethylene glycol as an active medium synchronously pumped by a mode-locked argon-ion laser (Spectra-Physics Model 171) was used to provide tunable pulsed excitation with a pulse duration of about 80 ps FWHM. The laser beam was attenuated by neutral glass filters to about 50 nJ per pulse at the sample. It should be pointed out that correct quantitative measurements of the fluorescence decay kinetics are only possible when the pulse-to-pulse separation in the excitation pulse train is substantially longer than the longest luminescence decay time exhibited by the sample under investigation. Since the longest decay components of the CdSe/ZnS nanocrystal luminescence are in the range of 100 ns (see below), the repetition frequency of the cavity dumper was set to 817 kHz. Additionally, for improving the accuracy of time resolved anisotropy measurements, care must be taken to reduce as much as possible the insufficiently surpressed secondary pulses in the instrument response function.

A Babinet–Soleil compensator was used to rotate the polarization of the exciting laser beam between the vertical (v) and horizontal (h) orientation. A vertically oriented film polarizer was used in the detection channel. Luminescence was spectrally selected after passing the analyzing polarizer using a grating monochromator (PTR Optics, Model SMC-02-22), with a spectral resolution of 3.5 nm. A Peltier-cooled R3809U microchannel plate-photomultiplier tube (MCP-PMT, Hamamatsu) was used as a fluorescence detector. A fast photodiode provided triggering pulses. The signal from the MCP-PMT was preamplified using a HFAC-26 amplifier (Becker & Hickl) and detected by a SPC-630 photon counting board (Becker & Hickl).

3. Analysis and results

3.1. Analytic procedure

When recording the PL intensity $I(t)$ with a vertical $I_{vv}(t)$ or a horizontal $I_{hv}(t)$ orientation of the polarization of the exciting beam, one can calculate the raw emission anisotropy $r_{\mathrm{raw}}(t)$ according to the formula

$$r_{\mathrm{raw}}(t) = \frac{I_{vv}(t) - GI_{hv}(t)}{I_{vv}(t) - 2GI_{hv}(t)}. \quad (1)$$

In the above notation for intensity decays, the first and second indices refer to the polarization orientation in the excitation and detection channel, respectively. The (positive) G-factor accounts for different luminescence excitation efficiencies for different polarizations of the exciting beam. We have found that in our set-up the deviations of the G-factor from unity were predominantly due to slow drifts in the laser power on time scales of 10–20 min. These variations did not exceed a few percent, and thus the experimentally determined G-factor is between 0.95 and 1.05. Typically, two or more luminescence decay traces were recorded at each detection wavelength for each polarizer orientation. Since the instrument response function is short enough, we were able to record the non-exponential excited state decay of the nanoparticles and the parameters of the

time resolved anisotropy were determined from the anisotropy decays. Stokes–Einstein–Debye (SED) theory was used to describe the rotational diffusion of nanoparticles in the solvent. According to the SED approach, the luminescence anisotropy should decay according to an exponential law

$$r(t) = r_0 \exp(-t/\theta), \tag{2}$$

with the rotational correlation time θ expressed by [16]

$$\theta = \frac{V\eta f}{k_B T} C, \tag{3}$$

where V is the solute volume, η the shear viscosity of the fluid, $k_B T$ the Boltzmann constant times the absolute temperature, f the factor accounting for the non-spherical shape of the solute, and C is a solute–solvent 'coupling parameter' [17]. In the analysis, we used the simple hydrodynamic theory of the rotational diffusion implying that $C = 1$. Additionally, the almost spherical shape of CdSe/ZnS nanocrystals allows us to set the factor f to unity with sufficiently high accuracy. Parameters r_o and θ of Eq. (2) were determined by a least-square analysis of the raw anisotropy (1). To improve accuracy, the G-factor was also fitted. It should be pointed out that the noise variances of the raw anisotropy data change substantially along the $r(t)$ curve. For this reason one should use a weighted least-square minimization [18], i.e. to approach the parameters of Eq. (2) by minimizing the weighted sum of squared residuals (WSSR) over M data points resulting in

$$\mathrm{WSSR} = \sum_{i=1}^{M} \frac{(r_{\mathrm{raw}}(t_i) - r_{\mathrm{model}}(t_i))^2}{\mathrm{var}\{r_{\mathrm{raw}}(t_i)\}}. \tag{4}$$

The following expression for the variance of the raw anisotropy value was obtained by assuming that var $\{I_{xv}(t_i)\} = I_{xv}(t_i)$, where $x = v$, h, which corresponds to a Poisson statistic of the TCSPC data and results in:

$$\begin{aligned}\mathrm{var}\{r_{\mathrm{raw}}(t_i)\} &= \frac{9G^2(I_{hv}^2(t_i)\mathrm{var}\{I_{vv}(t_i)\} + I_{vv}^2(t_i)\mathrm{var}\{I_{hv}(t_i)\})}{(I_{vv}(t_i) + 2GI_{hv}(t_i))^4} \\ &= \frac{9G^2 I_{vv}(t_i) I_{hv}(t_i)(I_{vv}(t_i) + I_{hv}(t_i))}{(I_{vv}(t_i) + 2GI_{hv}(t_i))^4}.\end{aligned} \tag{5}$$

With proper weighting the reduced χ^2 values for the raw anisotropy fits typically did not exceed 1.1, which is in good agreement between model and data, since the expected value of the reduced χ^2 should be in the optimum case close to 1.0 [18]. The accuracy of the anisotropy r_o and anisotropy decay time θ, as determined from the analysis of independent measurements, was about 0.002 and 5 ns, respectively.

3.2. Anisotropic photoluminescence decay

As is evident from Fig. 1, where the polarization resolved PL components are presented together with the polarization-insensitive excited state decay $I(t) = I_{vv}(t) + 2GI_{hv}(t)$, the luminescence decay of CdSe/ZnS nanocrystals is non-exponential. Clearly, the difference between the polarization resolved components is indicative of a non-negative anisotropy of the emission of an ensemble of nanocrystals. Moreover, it is obvious that the anisotropy decreases on approximately the same time scale as the excited state population. This is clearly seen in Fig. 2, where PL decay curves are compared with the raw photoluminescence anisotropy calculated from the experimental data. Fig. 2b shows that Eq. (2) qualitatively describes the observed time behaviour of the PL anisotropy (Fig. 2c) within experimental error. Similar results were obtained for all investigated combinations of excitation/emission wavelengths.

Time resolved PL anisotropy measurements were performed under identical conditions for excitation wavelengths at 575, 585, and 595 nm while detecting at a series of emission wavelengths, including the anti-Stokes region. The results are presented in Fig. 3, from which it is evident that within the experimental accuracy the anisotropy correlation time θ does not show a systematic dependence on the excitation and emission wavelength, and becomes $\theta = 40 \pm 5$ ns. On the contrary, the anisotropy r_o clearly shows a resonant behaviour with a maximum close to the respective excitation wavelength and decreasing towards the blue and red slopes of the emission spectrum. As is also evident from Fig. 3, the resonant behaviour of the initial anisotropy becomes

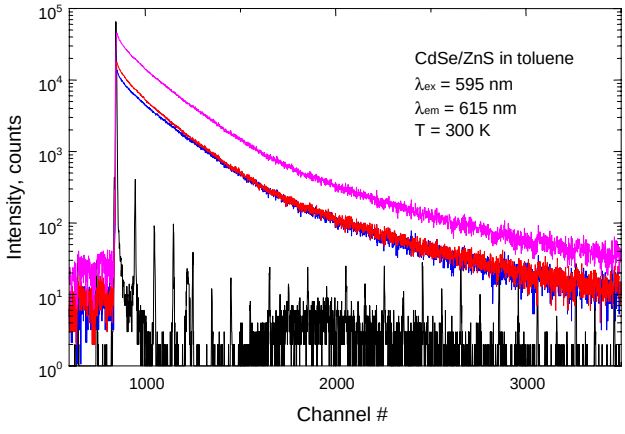

Fig. 1. Time resolved photoluminescence intensity traces $I(t) = I_{vv}(t) + 2GI_{hv}(t)$, $I_{vv}(t)$ and $GI_{hv}(t)$ (from top to bottom) of CdSe/ZnS nanocrystals. The instrument response function is also included. Resolution of the multichannel analyzer is 0.122 ns/channel. *Note*: The apparent background level at times preceeding the excitation pulse is due to the unsurpressed leakage from the cavity dumper.

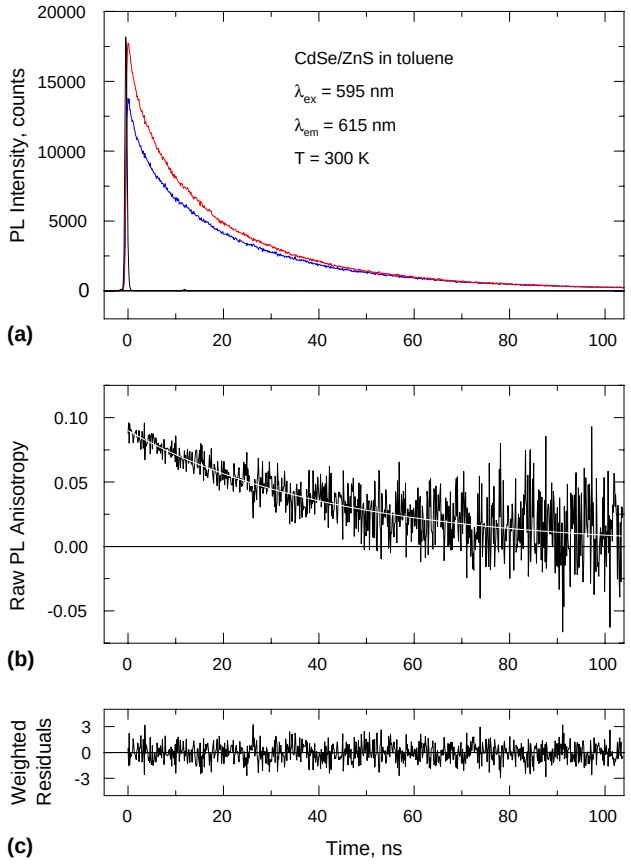

Fig. 2. Photoluminescence intensity and anisotropy decay of CdSe/ZnS nanocrystals. (a) Short time part of the decay traces $I_{vv}(t)$ (top) and $GI_{hv}(t)$ (bottom), as in Fig. 1 but on (b) photoluminescence anisotropy r_{raw} as calculated from the intensity decay according to Eq. (1) along with the fit according to Eq. (2). Parameters obtained from the fit are $r_o = 0.089$, $\theta = 43.0$ ns, and $G = 1.065$. (c) Weighted residuals of the fit with a reduced χ^2 of 1.024.

less pronounced with increasing excitation wavelength. Note that the maximum values of the anisotropy r_o are close to 0.1.

4. Discussion

To understand the behaviour of θ and r_o with respect to λ_{ex}, we have to discuss the origin of the anisotropic lineshape of the static PL of CdSe/ZnS. Due to quantum confinement the linewidth strongly depends on the diameter of the CdSe core which will thus determine the exciton band position. Since there is obviously a spread of sizes for CdSe crystals the rotational diffusion should reveal different rotational correlation times when tuning the excitation wavelength. Upon tuning the excitation to short wavelengths the correlation time θ should become faster since particles corresponding to these wavelengths are smaller. However, the experimental error is too large to draw definite conclusions.

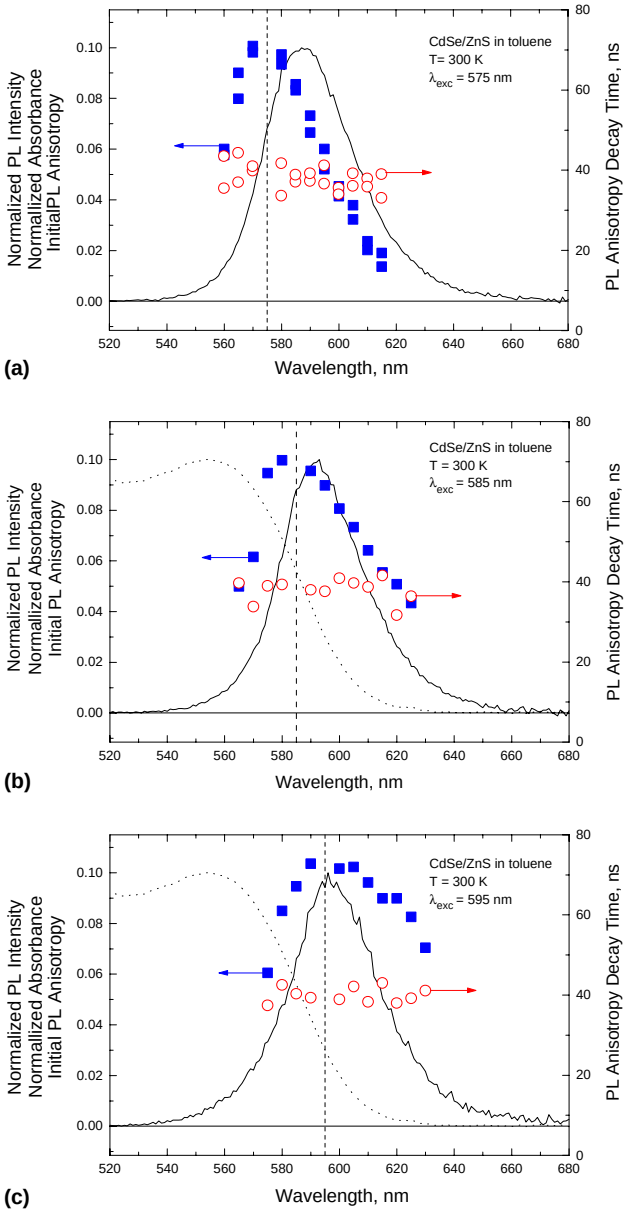

Fig. 3. Limiting (time-zero) PL anisotropies r_o (■) and corresponding anisotropy decay times θ (○) of CdSe/ZnS for three different excitation and various emission wavelengths. For clarity, the normalized (···) absorption spectrum and the steady-state PL emission spectra (—) for the corresponding excitation wavelength are also included. Vertical dotted lines mark the excitation wavelength λ_{ex}. (The panel for $\lambda_{ex} = 575$ nm shows results of two independent measurements to demonstrate data reproducibility.)

We further have to explain the resonance like behaviour of r_o which peaks at the correspondent excitation wave length. Fig. 3 also includes the PL spectra as obtained for the different excitation wavelengths. Since CdSe/ZnS crystals exhibit a remaining size distribution varying the excitation wavelength will result in a kind of spectral selection. At short excitation wavelength those particles will be excited which are corresponding to their respective size in resonance with the excitation

wavelength. Additionally, also those particles of the same size will be excited (to hot phonon bands) which are in thermally populated phonon ground states. Moreover, excitation will also occur into phonon bands of those particles for which corresponding to their (larger) size resonant exciton excitation will not be possible. Further on, those (smaller) particles will be excited to their correspondent zero phonon states which are in a thermally populated phonon state of the electronic ground state.

Shifting the excitation to longer wavelengths will reduce the relative contribution of hot phonon bands and limit the excitation to resonant exciton excitation of (large) particles and ground state populated phonon states of small particles. Since excitation of hot phonon states is accompanied by a fast radiationless transition (to the exciton ground state), PL from those states is strongly suppressed. This implies that PL can only be detected from the excited exciton ground state. For this reason the PL at short excitation wavelengths (containing noticeable excitation of hot but not emissive phonon states) is shifted to with respect to λ_{ex} longer wavelengths, whereas exciting at long wavelengths will result in with respect to λ_{ex} 'resonant' PL. As can be seen from Fig. 3, the PL peak shifts from 588 to 598 nm while tuning λ_{ex} from 575 to 595 nm.

How does the behaviour of r_o relate to λ_{ex} and λ_{em}? As can be seen from Fig. 3, r_o always peaks at that λ_{em} which is resonant with the corresponding λ_{ex}, but drops both to shorter and longer emission wavelengths. This effect is most pronounced for $\lambda_{ex} = 575$ nm, where r_o drops from 0.1 at maximum to atmost 0.01, while the change for λ_{ex} at 595 nm is only from 0.1 to 0.06. Moreover, the 'lineshape' of r_o is very asymmetric. The 'decay' is larger at long λ_{em} for $\lambda_{ex} = 575$ nm (small particle limit) and vice versa for $\lambda_{ex} = 595$ nm (large particle limit). For a homogeneous line shape r_o would be independent of λ_{ex} and λ_{em}. Exciting at short wavelengths, part of the nanocrystals will be as already discussed excited into a phonon state. Thus also 'hot' molecules are excited which will result in deviations from the expected Brownian diffusion process. Also those nanocrystals will be excited which are in a thermally populated phonon ground state, resulting in a similar effect upon r_o.

On the other hand, shifting the excitation to longer wavelengths less and less 'hot' nanocrystals will be excited till finally only resonance excitation of excitons will prevail and result in a constant r_o for a nearly homogeneous line shape. This behaviour is tentatively observed in the experiment. Also the asymmetry behaviour is in an overall agreement with the above arguments based on size selective excitation.

After having discussed the qualitative behaviour of the anisotropy decay times θ and the anisotropy value r_o we finally like to dwell on the absolute values of these parameters and relate it to structure and shape of CdSe/ZnS. Since CdSe/ZnS nanocrystals have an almost spherical shape, the non-spherical factor f can be set to unity with sufficient accuracy. Therefore, within the framework of the simple hydrodynamic theory for rotational diffusion ($C = 1$) and by taking into account that the viscosity of toluene is 0.55 cP [19] at 300 K, and with the experimentally determined rotational correlation times in the range of ~35–45 ns, we immediately obtain nanoparticle radii in the range of 4.0–4.3 nm. This result is in fair agreement with the parameters for the nanocrystals according to the preparation procedure, that is of $R = R_{CdSe} + 3d_{ZnS} = 1.6\ \text{nm} + 3 \times 0.5\ \text{nm} = 3.1\ \text{nm}$. The agreement becomes better if one recalls that TOPO molecules attached to the nanoparticle surface will increase the effective radius of the nanoparticle by about 1.0 nm to $R = 4.1$ nm.

Considering an isotropic 2D transition dipole, one would expect that the initial anisotropy of an ensemble of isotropically distributed nanocrystals will not exceed the value of 0.1. From photophysics of complex organic molecules this situation is well known for fluorescent molecules with high symmetry, such as coronene whose anisotropy value r_o is exactly 0.1 [20]. An elliptic shape will lead to slightly higher values of r_o in the range of 0.1–0.4, the higher limit being the limiting anisotropy for a 'normal' 1D transition dipole.

The anisotropy values r_o observed in our experiments clearly demonstrate a resonant behaviour, approaching values of almost 0.1 close to the excitation wavelength and decreasing towards both shorter and longer wavelengths. At the same time, the resonant behaviour becomes substantially less pronounced when increasing the excitation wavelength. This can tentatively be explained by assuming that Stokes or anti-Stokes shifted emission originates from excitons which gained or lost energy upon interaction with phonons. As the anisotropy of an ensemble equals the sum of anisotropies of subensembles and taken into account their relative contributions, the shapes of the anisotropy of r_o will reflect the shape of the 'homogeneous' emission spectrum. Upon red-edge excitation, the largest contribution comes from resonantly excited nanocrystals, which leads as discussed above and observed in the experiment, to a flattening of the limiting anisotropy spectrum. More detailed experiments of the data are, however, required to interpret the observed phenomena on a completely quantitative level.

5. Conclusions

In conclusion, our experimental results show that PL of CdSe/ZnS nanocrystals in toluene at room temperature shows a time dependent anisotropy, whose time behaviour is consistent with the parameters of Brownian rotational motion of nanocrystals in an isotropic liquid. Comparing with low temperature data structure and

related electronic states are obviously not changed at high temperatures. The anisotropy r_o shows a pronounced resonant behaviour peaking at the corresponding excitation wavelength and is decreasing both towards longer and shorter emission wavelengths. The change in the character of the resonant behaviour of the anisotropy r_o with excitation wavelength is indicative of an enhanced photoselection within in the size distribution of nanocrystals upon excitation at the red-edge of the absorption spectrum. Details of self-aggregated nanoassemblies between CdSe/ZnS and porphyrine dyes will be described elsewhere [21].

Acknowledgements

The work has been supported by DFG grants for E.P.P. (SP392) and D.S. (RE1291). Helpful discussions with S. Gaponenko, Minsk, are gratefully acknowledged. Nanocrystals are a gift of A. Rogach, Department of Physics, LMU Munic and Dr. D.V. Talapin, Institute of Physical Chemistry, University of Hamburg, which is gratefully acknowledged.

References

[1] A.L. Efros, Phys. Rev. B 46 (1992) 7448.
[2] S.A. Empedocles, R. Neuhauser, K. Shimizu, M.G. Bawendi, Adv. Mater. 11 (1999) 1243.
[3] S.A. Empedocles, R. Neuhauser, M.G. Bawendi, Nature 399 (1999) 126.
[4] F. Koberling, U. Kolb, I. Potapova, G. Philipp, Th. Basché, A. Mews, J. Phys. Chem. B (2003) 7463.
[5] I. Chung, K.T. Shimizu, M.G. Bawendi, Proc. Natl. Acad. Sci. USA 100 (2003) 405.
[6] E. Johnston-Halperin, D.D. Awschalom, S.A. Crooker, Al.L. Efros, M. Rosen, X. Peng, A.P. Alivisatos, Phys. Rev. B 63 (2001) 205309.
[7] D.F. Underwood, T. Kippeny, S.L. Rosenthal, J. Phys. Chem. B 105 (2001) 436.
[8] J.R. Lakowicz, I. Gryczynski, Z. Gryczynski, C.J. Murphy, J. Phys. Chem. B 103 (1999) 7613.
[9] D.V. Talpin, A.L. Rogach, A. Kornowski, M. Haase, H. Weller, Nano Lett. 2 (2001) 207.
[10] O. Schmelz, A. Mews, T. Basché, A. Herrmann, K. Müllen, Langmuir 17 (2001) 2861.
[11] J.A. Gardecki, M. Maroncelli, Appl. Spectrosc. 52 (1998) 1700.
[12] J.N. Demas, G.A. Crosby, J. Phys. Chem. 75 (1971) 991.
[13] K.H. Drexhage, J. Res. Natl. Bur. Stand. 80A (1976) 421.
[14] T. Karstens, K. Knobs, J. Phys. Chem. 84 (1980) 1871.
[15] P.J. Sadowski, G.R. Fleming, Chem. Phys. Lett. 57 (1978) 526.
[16] G.T. Evans, D. Kivelson, J. Chem. Phys. 84 (1986) 385.
[17] F. Kivelson, B. Kowert, J. Chem. Phys. 64 (1976) 5206.
[18] P.R. Bevington, D.K. Robinson, Data Reduction and Error Analysis for the Physical Sciences, second ed., McGraw-Hill, New York, 1994.
[19] J.A. Riddick, W.B. Bunger, T.K. Sakano, Organic Solvents, Wiley, New York, 1986.
[20] J.R. Lakowicz, Principles of Fluorescence Spectroscopy, second ed., Kluwer Academic/PLenum, New York, 1999.
[21] E. Zenkevich, F. Cichos, A. Shulga, E. Petrov, T. Blaudeck, C. von Borczyskowski, J. Phys. Chem. B, in press.